

NUMERICAL ANALYSIS OF STRENGTHENED MASONRY STRUCTURES DUE TO SUBSOIL DEFORMATION

Leszek SZOJDA*

^aDSc; Faculty of Civil Engineering, The Silesian University of Technology, Akademicka 5, 44-100 Gliwice, Poland
E-mail address: leszek.szojda@polsl.pl

Received: 15.10.2012; Revised: 15.12.2012; Accepted: 15.12.2012

Abstract

The paper presents the numerical analysis of a masonry building subject to the influence of ground deformation. Numerical analysis was carried out by elastic-plastic material model. The shape of the boundary surface was adopted from three parameter Willam-Warnke criterion. The calibration of the boundary surface shape has been carried out in the course of laboratory tests of masonry samples subjected to compression and shear loading. The numerical analyses were carried out by the heterogeneous as well as the homogeneous materials model. The results of the buildings numerical analysis were compared with a real building and gave satisfactory compatibility. Use of structure strengthening resulted in reduction of the elements effort level. However, it was not fully possible to avoid damage due to only partial structure strengthening. Some quantitative differences in the results between analytical model and the real structure, which was caused by difficulties in defining the parameters of an existing material of masonry have also be noted.

Streszczenie

Artykuł przedstawia analizę numeryczną murowanego budynku mieszkalnego poddanego wpływowi deformacji terenu. W analizie numerycznej wykorzystano sprężysto-plastyczny model materiałowy. Kształt powierzchni granicznej została zaadaptowana z trójparametrowego kryterium Willam-Warnke. Kalibracja kształtu powierzchni granicznej została przeprowadzona na podstawie testów laboratoryjnych próbek murowych poddanych obciążeniom ściskającym i ścinającym. Obliczenia prowadzone były dla heterogenicznego, jak i homogenicznego modelu materiałowego. Wyniki analizy numerycznej obiektu zostały porównane z budynkiem rzeczywistym i dały satysfakcjonującą zgodność. Użycie elementów wzmacniających spowodowało obniżenie poziomu wyężenia elementów. Nie udało się jednak całkowicie uniknąć uszkodzeń budynku ze względu na częściowe wzmocnienia. Zostały również zauważone ilościowe różnice naprężeń pomiędzy rezultatami analizy numerycznej, a rzeczywistą konstrukcją, co było spowodowane trudnościami w zdefiniowaniu parametrów materiałowych istniejącego muru budynku.

Keywords: Boundary surface; Elastic-plastic material model; FEM analysis; Ground deformation; Masonry structure.

1. INTRODUCTION

Brick wall residential buildings have long tradition of erection. This structural material was particularly often used in the region of rapid industrial development during early years of the last century. The development was significant in Upper Silesia too. In the second half of the last century the importance of brick wall structure decreased in favour of reinforced concrete structures (precast flats buildings). Nevertheless in the last decades brick wall structures experience renaissance of use.

The region of the Upper Silesia is very rich in hard coal source. The excavation of coal on industrial scale caused significant ground deformation in the places, where the buildings are settled. The deformations of the ground are transmitted to the structure causing different failures from not significant cracks to destruction of the structure. Prediction of the failure structure could be carried out by means of natural scale laboratory tests or appropriate numerical analysis which allowed to decrease the costs. Important attribute of numerical analyses is adequate material

model of the calculation as well as possibility of different materials use (mortar, brick, concrete, steel, soil). In this conditions the calculations can point out the most threatened region in the structures and allowed to improve the structure by putting the strengthening elements into the structure.

The development of computational methods allows to carry the analysis of complex structural problems. The use of appropriate material model for numerical analysis is necessary to achieve proper representation of reality. A numerical analysis of the real apartment masonry building, which has been subjected to the influence of the subsoil deformation of high intensity (discontinuous deformation) is presented below. For numerical calculations an elastic-plastic material model with material softening was used. For the description of numerical material model a boundary surface was applied. This surface was determined by Willam-Warnke three parametrical criterion [1] with modification made by Prof. S. Majewski [2]. The correctness of theoretical assumptions was compared with the laboratory tests of compression and shear masonry specimens. Creation of a suitable model material with proper parameters calibration allows to carry out the analysis of complex structures without necessity of building expensive laboratory stands. The example of numerical analysis was presented below to determine the effectiveness of traditional building protection in the case of additional loads significantly exceeding the expected level and type.

2. MATERIAL MODEL

Description of material model was presented in detail on previous AMCM conference in 2008 [1]. In initial analysis the elastic-plastic and elastic-brittle material models were taken into consideration. These assumptions modelled a material behaviour for brick and mortar in complex stress state in the best way. The material tests were carried out in multi-axial apparatus, which enabled the definition of main meridians of boundary surface.

2.1. Elastic-plastic material model

The basic assumption of elastic-plastic material model is the assumption of suitable relationship between stress and strain. For brick and mortar isotropic material properties were also assumed, which can reduce the number of variables defining the constitutive relations (initial value of elastic modulus E_0 and Poisson's coefficient ν_0). During the load

and at the same time stress increase, the strains grow in both elastic and plastic material work phase. For each material there is a certain stress level at which the material deforms only plastically. In case of the materials taken into consideration this phenomenon occurs in a very short period of loading and relatively quickly a damage or substantial permanent deformation of the material arises (in case of significant compressive normal octahedral stress), or in the form of crack distribution (damage is determined by difference of principal stresses at low level of normal octahedral stress). Assumptions made for the mortar and bricks have been modelled on the assumptions adopted for the concrete, which were presented in detail by S. Majewski [2]. In further analyses coincidence of plastic and boundary surfaces were assumed, which means that the materials do not sustain the isotropic hardening. These types of assumptions for the concrete were presented by Chen [3], [4], Bažant [5] and Godycki-Ćwirko [6].

Boundary surface determined for the concrete and presented by S. Majewski is based on the determination of the two main meridians. They consist of rectilinear part in mean normal octahedral compressive stress and tangential parabolic caps in small compressive and tensile normal octahedral stress. The stress relations were described in octahedral stress space and were given by normal σ_{oct} and shear τ_{oct} octahedral stress, Lode angle θ in formulas (1) to (5).

$$\sigma_{oct} = \frac{\sigma_x + \sigma_y + \sigma_z}{3} \quad (1)$$

$$\tau_{oct} = \frac{1}{3} \sqrt{(\sigma_x - \sigma_y)^2 + (\sigma_y - \sigma_z)^2 + (\sigma_z - \sigma_x)^2 + 6(\tau_{xy}^2 + \tau_{yz}^2 + \tau_{zx}^2)} \quad (2)$$

$$J_2 = \frac{2}{3} \tau_{oct}^2 \quad (3)$$

$$J_3 = \begin{vmatrix} \sigma_x - \sigma_{oct} & \tau_{xy} & \tau_{xz} \\ \tau_{yx} & \sigma_y - \sigma_{oct} & \tau_{yz} \\ \tau_{zx} & \tau_{zy} & \sigma_z - \sigma_{oct} \end{vmatrix} \quad (4)$$

$$\cos 3\theta = \frac{3\sqrt{3}}{2} \frac{J_3}{J_2^{3/2}} \quad (5)$$

The main meridians appear in the octahedral stress space within the period specified by the relation (6) and (7), in the deviatoric cross-section at 60° will occur compression and tensile meridian. The relation was described in principal stresses and the main

meridian was been achieved by stress vector when the principal stresses (loading path) fulfil the condition:

$$\Theta = 0^\circ + \frac{2\pi}{3} \quad \text{for } \sigma_1 = \sigma_2 < \sigma_3 \quad (6)$$

compressive meridian

$$\Theta = 60^\circ + \frac{2\pi}{3} \quad \text{for } \sigma_1 = \sigma_2 > \sigma_3 \quad (7)$$

tensile meridian

The construction of the surface fitting the all meridians was proposed by Willam-Warnke [1]. The description of the boundary surface between main meridian was given by radius $r(\theta)$ related to uniaxial compressive f_c and tensile f_t strength (8) and (9).

$$\rho(\theta) = \frac{2(1-\rho^2)\cos\theta + (2\rho-1)\sqrt{4(1-\rho^2)\cos^2\theta + 5\rho^2 - 4\rho}}{4(1-\rho^2)\cos^2\theta + (1-2\rho)^2} \quad (8)$$

$$\rho = \frac{3f_{cc}f_t + f_c(f_{cc} - f_t)}{f_c(2f_{cc} + f_t)} \quad (9)$$

$$r(\theta) = r_c \rho(\theta) \quad (10)$$

Crossing by plane containing both main meridians and trace of the meridians in deviatoric cross-section were shown in Figure 1 and the relation of radius in deviatoric cross-section was presented in Figure 2.

Masonry wall material (brick and mortar) were tested and it allowed to define the main meridian. These meridians defined in stress space contain characteristic points – uniaxial compression strength f_c (compression meridian), strength of the state of uniaxial tensile strength f_t and biaxial compression strength f_{cc} (tensile meridian). These points allow you to adapt the shape of the surface of the same materials, but with slightly different parameters.

2.2. Boundary surface for material model

The defined above surface was described in detail in the space of stresses due to multi-axial compression tests. The tests were made on cylindrical specimens for mortar and brick in a monotonic way. The dimensions of cylinder were – diameter 60 mm and height 120 mm. The damage of the material took place at two different stress relations. The first covered the loading path where the destructive stress was applied in a parallel direction to the axis of the cylinder with different levels of compressive stresses on the side

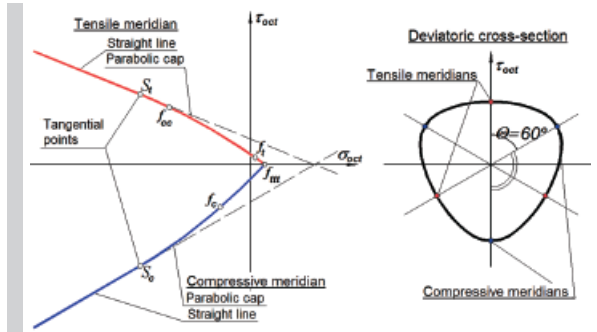


Figure 1. Boundary surface in main meridian and deviatoric cross-section

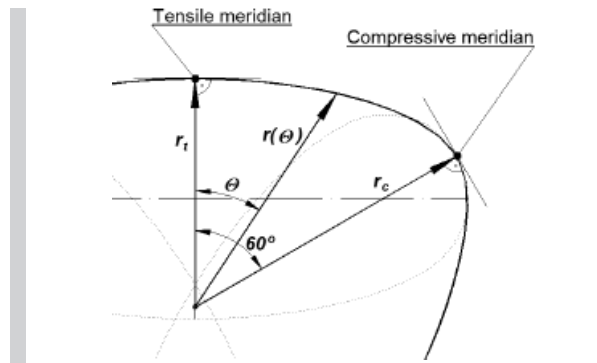


Figure 2. The radius relation $r(\theta)$ between main meridians

surface of the cylinder. A special case of the loading occurs when the side surface stresses equal zero. This case gives uni-axial compressive strength for material f_c . The results of the specimens tests were presented in [7]. All test results for such loading paths are focused along the compressive meridian.

The second type of the loading path assumed the destruction of the specimens by side surface compressive stress increasing at different levels of constant stress on the base of the cylinder. The special case of this loading path appears when the damage stresses were provided on the side surface at lack of stress on the cylinder bases – biaxial compressive strength f_{cc} . The results of these tests are focused along the tensile meridian.

Detailed results of laboratory tests were presented in a paper at the previous conference [8]. Rectilinear and parabolic part of the main meridians for both materials describe the values given in Table 1.

Table 1.
Parameters of boundary surfaces main meridians

		Brick meridians		Mortar meridians	
		compressive	tensile	compressive	tensile
Parabolic cap $\frac{\tau_{oct}}{f_c} = A \left(\frac{\sigma_{oct}}{f_c} \right)^2 + B \frac{\sigma_{oct}}{f_c} + C$	A	0.6955	-0.4294	0.1750	-0.1204
	B	0.9490	-0.5858	0.9900	-0.6817
	C	-0.2324	0.1434	-0.1608	0.1108
Rectilinear part $\frac{\tau_{oct}}{f_c} = a \frac{\sigma_{oct}}{f_c} + b$	a	0.6589	-0.4067	0.5871	-0.4044
	b	-0.2626	0.1621	-0.3928	0.2704

For easier application of the boundary surface for slightly different material (e.g. brick from different batch or different mortar mixes) the relationship in coordination system was performed in dimensionless units. It means that the values of normal σ_{oct} and tangential τ_{oct} , octahedral stress and the accompanying Lode angle θ were divided by uniaxial compression strength f_c of the described material. This assumption enables the application of defined boundary surface for different testing material in further laboratory tests. Fig 3 and 4 present the main meridians for

bricks and mortar in the space of octahedral stresses. Note, that the main meridians of boundary surface were presented in unit-less coordination system – normal octahedral stress σ_{oct} and shear octahedral stress τ_{oct} are divisible by uniaxial compression strength f_c for each material.

3. LABORATORY VERIFICATION OF THE MATERIAL MODEL

Verification of the proper material model in the form of suitable boundary surface was carried out by means of laboratory tests, which were made by Prof. J. Kubica [9], [10] in the Civil Engineering Laboratory of the Silesian University of Technology. The laboratory tests included masonry specimens compression and shear experiments. Material parameters used in the numerical analysis have been applied from the accompanying laboratory tests of the masonry specimens.

3.1. Compression tests of the masonry specimens

Compression tests of masonry were carried out with the use of specimens of dimensions 510x665x120 mm and the test was made under force control. The specimens were made of solid ceramic bricks and cement-lime mortar. The specimen was modelled in non-commercial software Mafem3D (author Prof. S. Majewski). The division of the specimen into the finite elements was performed along the surface of the material, so one finite element includes only one material – mortar or brick. Due to the nature of the experience the computational model consisting of 1/8 of the whole laboratory specimen only because of the three planes of symmetry. The dimensions of the finite element ranged from 5mm to 16.25 mm (four items at the height of brick). With such dimensions

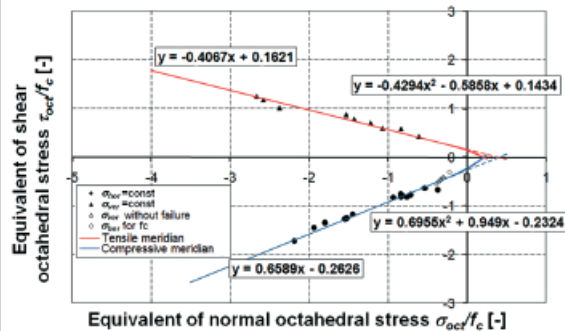


Figure 3.
Main meridian of boundary surface for brick

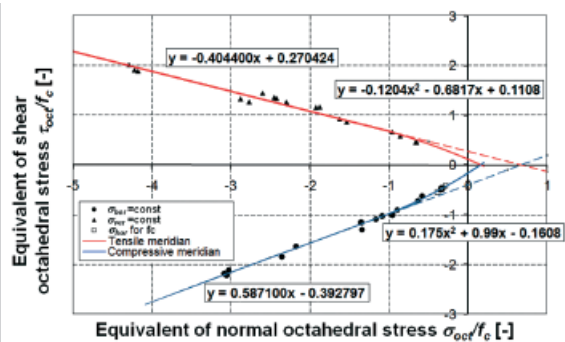


Figure 4.
Main meridian of boundary surface for mortar

the numerical model consisted of 2660 nodes and 1944 solid elements. The compression load was applied to the upper surface of the specimen and implemented as a displacement, divided into 41 steps. The total displacement was taken at 2mm. Laboratory specimen and FEM model is presented in Figure 5. The results of the FEM analyses of compression tests are presented in [11].

Calculations were performed in two stages by analyzing the problem with the use of the material parameters of mortar and brick in finite elements (heterogeneous model) and the averaged material parameters

for all finite elements (homogeneous model). Average values of material parameters were obtained from mortar and brick parameters according to the dependence given by Gambarotta and Logomarsino [12].

During the experiments the loads, deformations and the origin and development of cracks were recorded. Deformation of laboratory model were controlled by measurement of distances between base points fixed on the lateral surfaces of the specimens in the shape of 260x300 mm rectangle. Node number 1591 of numerical model corresponded to the base point of specimen, which was used to compare numerical model strain. The detailed description of the numerical analysis results was presented in [1]. Figure 6 shows the comparison between strains of laboratory and numerical model for the parameters of hetero- and homogeneous material.

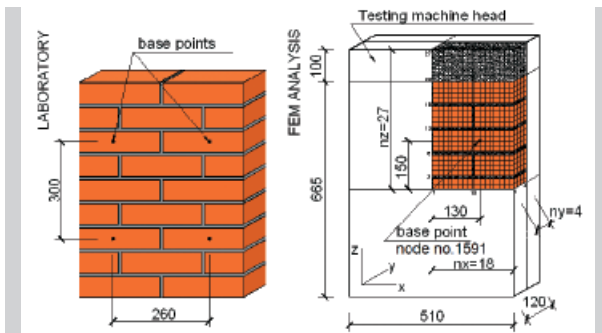


Figure 5. Lab specimen and FEM model in compression test

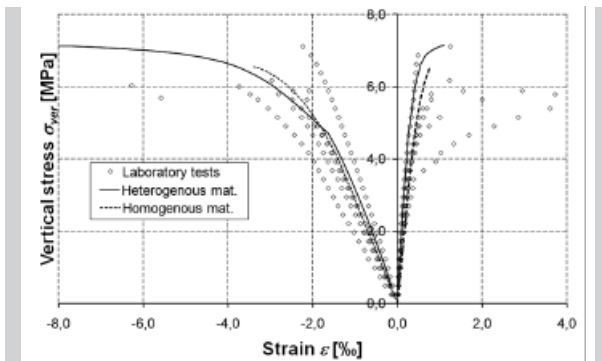


Figure 6. Stress-strain relation for lab specimen, hetero- and homogenous material model in compression test

3.2. Shear tests of the masonry specimens

The numerical analyses of shear tests was made on real laboratory tests too. Laboratory models were prepared of solid bricks and cement-lime mortar. The dimensions of tested specimens were 1420x1415x250 mm. The numerical analyses was also performed in Mafem3D. The numerical model consisted of half specimen due to one symmetry plane. The range of finite element dimensions was from 10mm to 55mm. The model consisted of 5130 nodes and 2464 solid elements. The load was attached along the vertical edge of specimens and was divided into 49 loading steps per 7.5kN in each to the maximum value of 367.5kN. Figure 7 shows the laboratory and numerical model of shear tests.

The numerical analysis of shear tests was carried out using of the heterogeneous and homogeneous material model as well as in compression tests. Material parameters used in numerical calculation were shown in Table 2.

Table 2. Material parameters for shear tests

Material parameter			Heterogeneous material		Homogenous material
			Brick	Mortar	
Uniaxial compression strength	f_c	MPa	-11.49	-7.39	-8.11
Initial value of elasticity modulus	E_o	MPa	7952.2	8555.7	8032.0
Initial value of Poisson coefficient	ν_o	-	0.062	0.161	0.075
Extreme strain for uniaxial compression $\sigma_{ve,max}$	σ_c	%	-2.00	-2.00	-2.60

Comparing the numerical analysis and laboratory tests results the strains and development of cracks were considered. The base points on lateral surface of masonry specimens were placed on the rectangle corners – 500x500 mm. These base points correspond to the location of the numerical model and were used to compare strains between laboratory specimen and computational model. Description of the numerical analysis was presented in [13] and [14]. Figure 8 represents the non-dilatation angle θ_A depending on the size of shear stress τ_{xz} , which appeared on vertical edge of specimen in laboratory specimen and numerical model under displacement control of the base point.

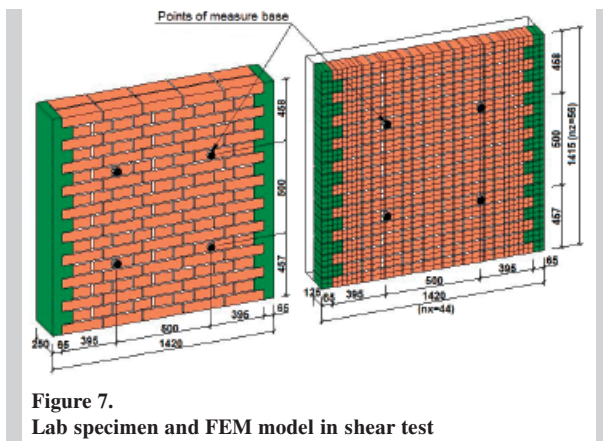


Figure 7. Lab specimen and FEM model in shear test

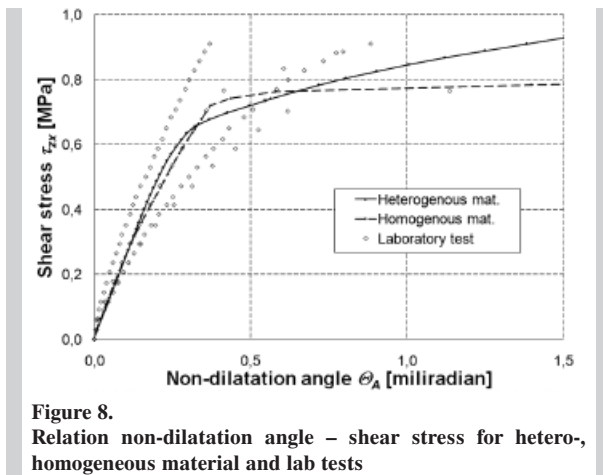


Figure 8. Relation non-dilatation angle – shear stress for hetero-, homogeneous material and lab tests

The assumed different values of material parameters for compression and shear tests were caused by the specific material parameters implemented to the laboratory models. The lab models were made of different brick batch and mortar mix. For this reason the averaged homogeneous material parameters are different and the softening effect was not observed

because the laboratory test and numerical analysis were provided under force control. Despite these difficulties the numerical analysis results coincide with the results of laboratory tests. It allowed to consider a similar scheme for determining of material parameters in the numerical analysis of a masonry building.

4. NUMERICAL MODEL OF ANALYSED BUILDING

The residential building, which was located on the mining area of one of the coal mines was subjected to numerical analysis. The building is a typical two-storey residential facility occurring in the Upper Silesia region. It was built in 1938, and the structural material is a masonry (solid brick) with lime mortar. The structure of floors and the roof is made of wood. The part of the building has a basement and the roof over the basement was made of steel beams (I cross-section). The dimensions of the building projection are similar to –10.53x10.98 m square at the height of the terrain around 9m. The walls thickness is varied and the basement level dimension is 510 mm (outer walls) and 380 mm (internal walls). The above ground part of the wall thickness is reduced to 380 mm and 250 mm respectively.

The building has been subjected to the subsoil deformation of continuous type (II level of land mines category) and discontinuous type – field ruffle about 5cm. The settled area included approximately 70% of the building projection. This effect was most significant in terms of damage to the building, which is presented by cracks in the building carrying walls. Also facility inclination up to 21‰ was a result of ground deformations. A detailed description of the damage has been presented in [11].

For the building described above numerical model was prepared. Calculations were made with the use of Mafem3D program. The division of the object into finite elements is shown in Figure 9. The assumed computational model consisted of 5340 nodes and 2389 solid elements. In the numerical model the floors and roof structure were omitted because of small stiffness of these elements, which does not affect the change of internal forces in the masonry walls. The parameters of masonry wall were taken as average values of properties – the parameters for homogeneous material. The values of material properties which were used for the analysis are presented in Table 3. The software Mafem3D uses the incremental-iterative method of load applying. The total number of calculation steps was 50. In the first steps

Table 3.
Material parameters for numerical analysis of the building

Material parameter			Heterogeneous material	Homogenous material
Uniaxial compression strength	f_c	MPa	-3,12	-8.11
Initial value of elasticity modulus	E_o	MPa	8032	8032.0
Initial value of Poisson coefficient	ν_o	-	0,075	0.075
Extreme strain for uniaxial compression $\sigma_{ver,max}$	σ_c	$\%$	-2,60	-2.60

of calculation the object was loaded by its own weight, operation loads (steps 1 to 5) and ground deformation corresponding to the formed field ruffle (steps 6 to 50). In order to take account of the impact-absorbing ground phenomena the support of the computational model was realized by means of vertical bars, which were inserted to each nodal point of the solid elements lowest layer. Material parameters of the support elements (bars) represented elastic modulus of soil $E_{o,gr} = 50$ MPa. The calculations did not consider in detail the behaviour of the soil, and the used material model was of linear elastic properties, which corresponds to the Winkler model assumptions. With such assumptions it was possible to take into account the large ground deformation in compression zone, and separate the foundation from the ground in case of tension.

The behaviour of the individual walls of the numerical model for the structure without reinforcement was presented in [11].

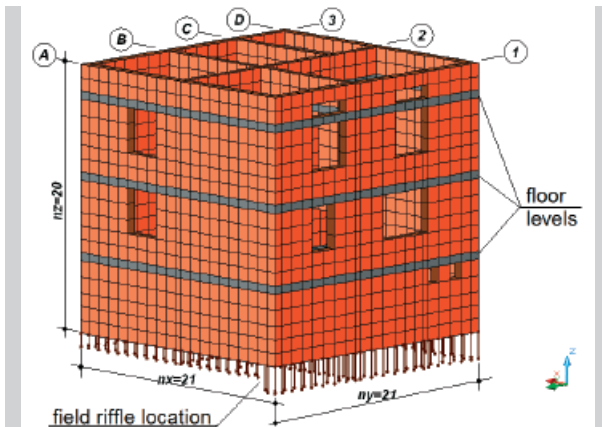


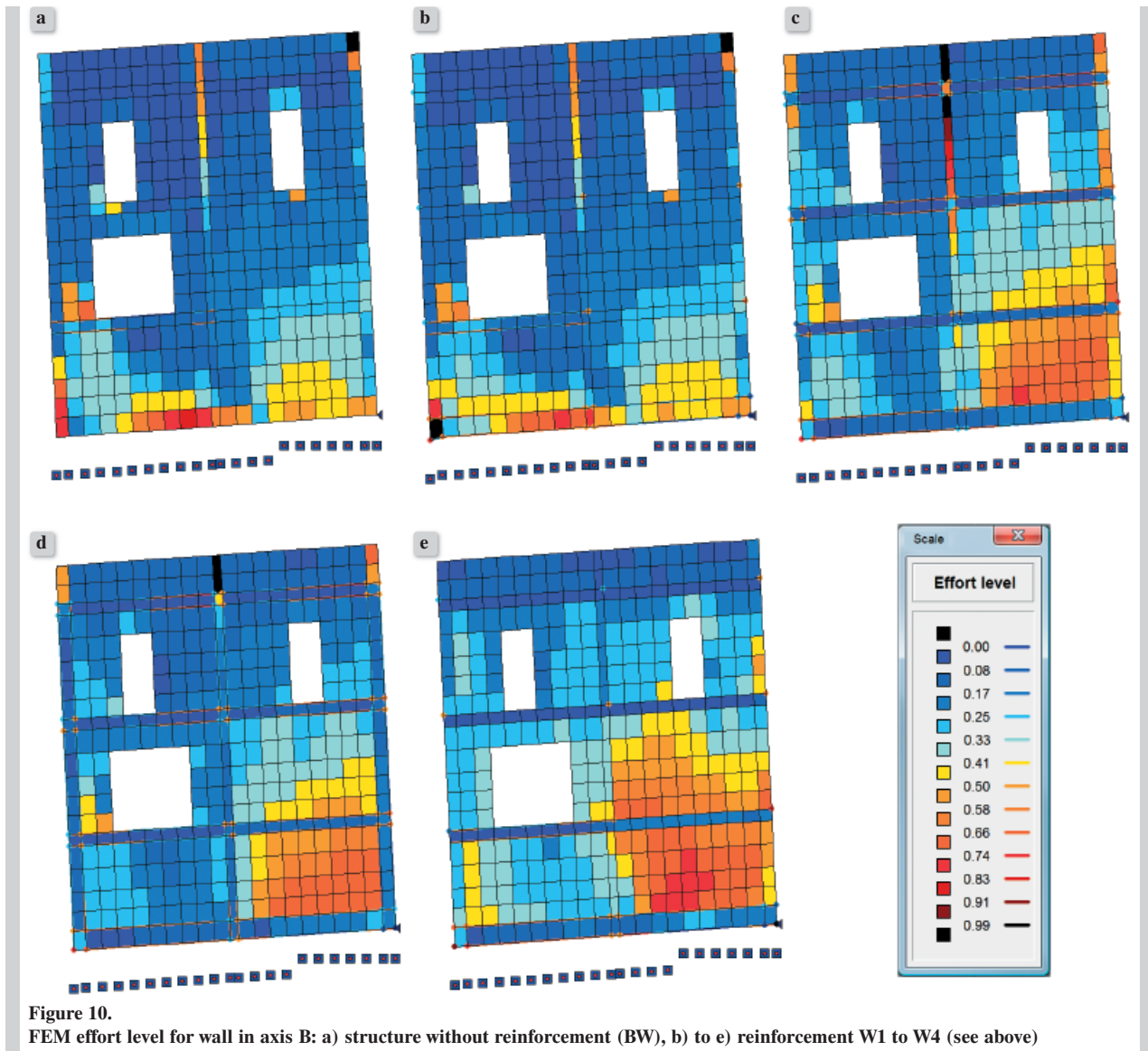
Figure 9.
FEM model of the analyzed apartment building

4.1. Description of building reinforcement

Using the numerical model of a residential building several reinforcements were included. The nature of reinforcements were similar to the recommendations of the buildings protection against the influence of continuous mining deformation. The numerical model changes were made to include four types of reinforcements, which respectively, changed the number of nodes, solid elements and bars:

- W1 reinforcement – steel tie rods at the ceiling level (single bar $\phi 25$ along carrying walls) + arm-band in the foundation level ($4\phi 25$ along carrying walls) – 5340 nodes, 2389 solid elements, 1390 bars (option implemented to strengthen the building)
- W2 reinforcement – curbs in the ceiling level ($4\phi 16$ along carrying walls) + reinforced concrete continuous footing ($4\phi 25$ along carrying walls) – 5340 nodes, 2389 solid elements, 2652 bars,
- W3 reinforcement – curbs in the ceiling level ($4\phi 16$ along carrying walls) + reinforced concrete continuous footing ($4\phi 25$ along carrying walls) and reinforced concrete cores in walls crossing between continuous footing and roof level ($4\phi 16$) – 5340 nodes, 2389 solid elements, 3444 bars,
- W4 reinforcement – replacement of the existing wooden ceiling of reinforced concrete slab (reinforcement of concrete slab $9\phi 12$ per meter, reinforced concrete curbs $4\phi 16$ in ceilings level, reinforced concrete continuous footing $4\phi 25$) – 6204 nodes, 2946 solid elements, 1434 bars.

The steel reinforcement of the building was modelled as rod elements between the nodes of the solid elements. The placed concrete elements did not change the shape of the numerical structure with the exception of the reinforcement W4 – concrete ceiling slabs.



4.2. Numerical analysis results

The analysis of numerical calculation results for different types of reinforcements was carried out by comparing the state of internal forces (effort levels) in the last 50th calculation step. The compared parameter was the level of effort in finite elements, which is defined as a value of the shear octahedral stress in the individual element $\tau_{oct,el}$ to the shear octahedral stress on the boundary surface $\tau_{oct,lim}$ at the same value of normal octahedral stress σ_{oct} and Lode angle θ . Exhaustion of the material element strength appears when the effort level reaches 1.0. The step change of the effort level appears on the wall surface in models with different materials (e.g. concrete reinforcement).

The following figures (Fig. 10 and 11) present changes of the effort level in the masonry walls in axes B and 1 for an object without reinforcement (BW) and additionally reinforcements (W1 to W4). The decrease of internal forces (the effort levels) is visible in the model with reinforcements. Lowering the effort level is proportional to the size of entered reinforcements. The best results of effort level reduction were achieved in reinforcement W4 – with reinforced concrete slabs and concrete cores between foundation and slabs curbs. It was presented in Figure 11a (model without reinforcement BW) and Figure 11e – reinforced W4.

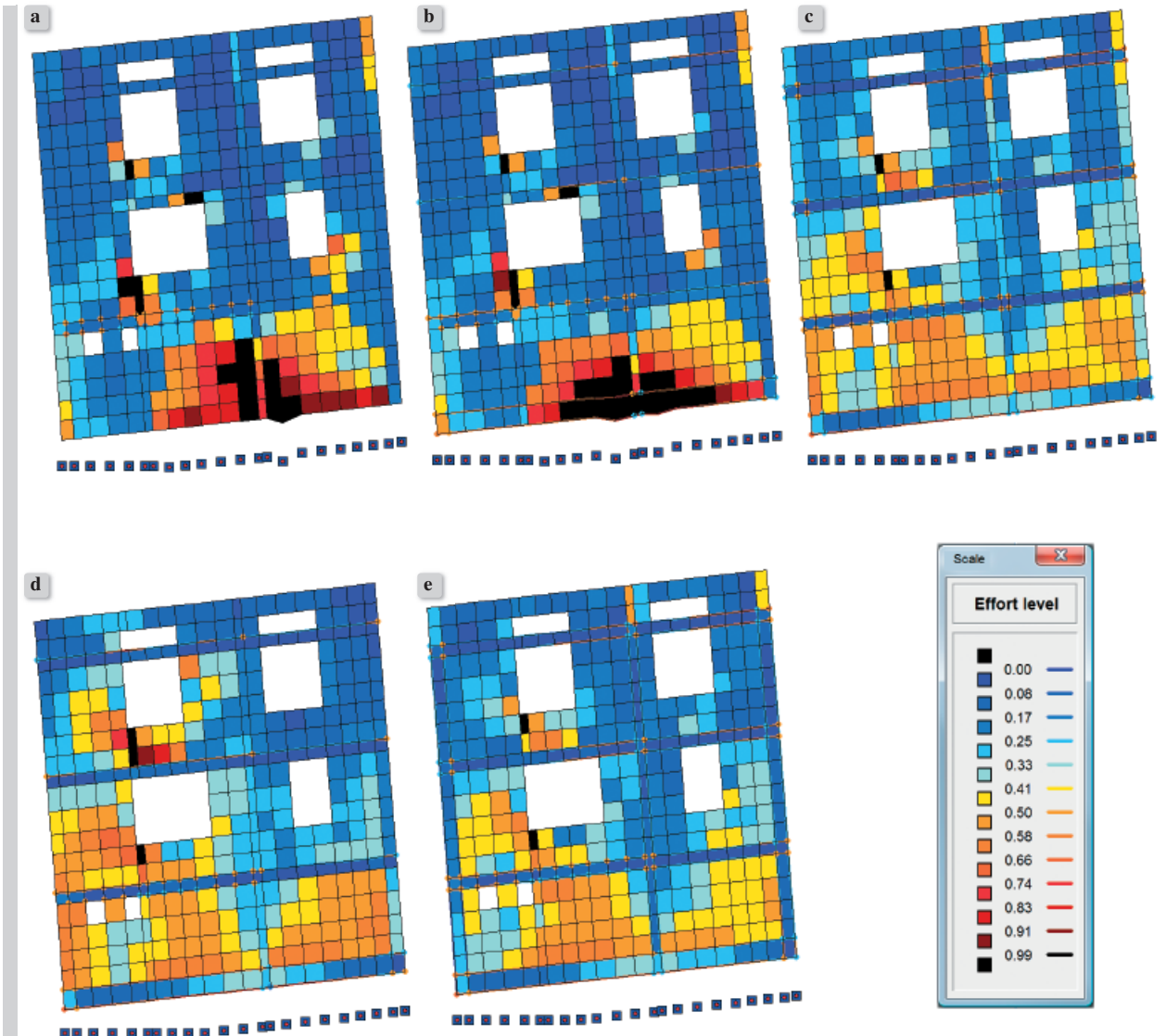


Figure 11. FEM effort level for wall in axis 1: a) structure without reinforcement (BW), b) to e) reinforcement W1 to W4 (see above)

5. SUMMARY AND CONCLUSIONS

In this paper the numerical analysis of the masonry structure subjected to the ground deformation was shown. The analysis was carried out by non-commercial software MAFEM3D made by Prof. Majewski. In numerical analysis the material model uses relation of boundary surface for all materials. The surface was created for concrete but following laboratory test it was possible to improve those relations for heterogeneous material (separately for mortar and brick) as well as for material with mean material parameters (called homogeneous material). Results of numerical calculations with both material properties (hetero- and homogeneous) were compared with the use of

laboratory compression and shear tests. Satisfactory agreement between lab tests and numerical analysis enabled the use of this homogeneous material model for numerical analysis of the whole structure of residential building. Modelled real structure was situated above ground fault (non-continuous ground deformation) which had the biggest influence on the structure. During the numerical analysis the structure was strengthened by additional RC element – continuous foundation, curbs on the ceilings level, vertical cores. The application of the elements enabled observation significant reduction of the principal stresses in finite elements of the structure walls.

The following conclusions can be drawn from the analyses:

- the applied material parameters of the building structure were not determined in detail because of the lack of material tests;
- reinforced elements in the structure were applied according to the recommendations of erecting buildings in mining areas with the continuous ground deformation but full protection of the building against discontinuous ground deformation is possible practically only for the brand new building;
- reinforcement elements introduced in the numerical model showed a reduction in the elements effort level, which indicates the desired impact on the overall structure;
- the results of numerical analysis of model without reinforcements confirmed the place of stress concentration, however, a level of stress, which would represent the places of damages (element depletion load) in place of actual damage to the building was not reached. This confirms the qualitative accordance of numerical analysis with the experiment. The less quantitative accordance was noted due to the lack of well defined material parameters of the masonry wall forming the real structure.

ACKNOWLEDGEMENTS

This paper was presented at the 7th Intern. Conf. on Analytical Models and New Concepts in Concrete and Masonry Structures (AMCM'2011), Krakow, June 2011

REFERENCES

- [1] *Willam K. J., Warnke E. P.*; Constitutive Models for the Triaxial Behaviour of Concrete. IABSE Seminar on Concrete Structures Subjected to Triaxial Stresses, Bergamo, IABSE Proc. Vol.19, 1974; p.1-30
- [2] *Majewski S.*; Mechanics of Structural Concrete In Terms of Elasto-plasticity. Wydawnictwo Politechniki Śląskiej, Gliwice 2003, p.186 (in Polish)
- [3] *Chen C. T., Chen W. F.*; Constitutive relation for concrete, Journal of Engineering Mechanics Division ASCE, Vol.101, 1975; p.465-481
- [4] *Chen W. F.*; Plasticity for Reinforced Concrete, McGraw-Hill Book Company, New York, 1982
- [5] *Bazant Z. P., Chern J. C.*; Log Double Power Law for Concrete Creep, ACI Journal, no.82, 1985; p.665-675
- [6] *Godzycki-Ćwirko T.*; Concrete Mechanics. Arkady Warszawa, 1982 (in Polish)
- [7] *Szojda L.*; Numerical analysis of influence of non-continuous ground displacement on masonry structures. Monograph. Wydawnictwo Politechniki Śląskiej, Gliwice 2009, p.194 (in Polish)
- [8] *Szojda L.*; Boundary surface of material model for brick and mortar as a result of multiaxial tests. 6th AMCM, 9-11 June 2008, Łódź Poland, p.365-366 and CD
- [9] *Kubica J., Majewski S., Starosolski W., Szojda L., Drobiec Ł., Jasiński R., Piekarczyk A.*; Load capacity and deformability analysis of brick-wall structure loaded by shearing perpendicular to bet-join caused by mining subsidence vertical deformation, Final Report of Research Project of State Committee for Scientific Research number nr 7 T07E 026 15, Gliwice 2001; p.133 (in Polish)
- [10] *Kubica J.*; Unreinforced masonry walls subjected to non-dilatational strains produced by irregular vertical ground displacements (in Polish). Zeszyty Naukowe – Budownictwo, Politechnika Śląska, z.96, Gliwice 2003; p.196
- [11] *Krzywoń R., Szojda L., Wandzik G.*; Numerical analysis of building subjected to the ground subsidence. 6th AMCM, 9-11 June 2008, Łódź Poland, p.331-332 and CD
- [12] *Gambarotta L., Logomarsino S.*; Damages models for the seismic response of brick masonry shear walls. Part II; the continuum model and its application. Earth. Eng. and Struct. Dynamics, Vol.26, 1997; p.441-462
- [13] *Szojda L.*; Elastic-plastic material model for brick-wall subjected to shear loading – numerical analysis versus laboratory tests. International Symposium on Plasticity and its Current Application “PLASTICITY’10”, 3-8 January 2010, St. Kitts and Nevis, p.295-297 and CD
- [14] *Szojda L.*; Numerical Analysis of Masonry Structures. 8th International Masonry Conference, 4-7 July 2010, Dresden, Germany, p.1009-1016